

Report

In Vitro Reconstitution of the Functional Interplay between MCAK and EB3 at Microtubule Plus Ends

Susana Montenegro Gouveia,¹ Kris Leslie,¹ Lukas C. Kapitein,² Rubén M. Buey,⁴ Ilya Grigoriev,¹ Michael Wagenbach,⁵ Ihor Smal,³ Erik Meijering,³ Casper C. Hoogenraad,² Linda Wordeman,⁵ Michel O. Steinmetz,⁴ and Anna Akhmanova^{1,*}

¹Department of Cell Biology

²Department of Neuroscience

³Biomedical Imaging Group Rotterdam, Departments of Medical Informatics and Radiology Erasmus Medical Center, PO Box 2040, 3000 CA Rotterdam, The Netherlands

⁴Laboratory of Biomolecular Research, Paul Scherrer Institut, CH-5232 Villigen PSI, Switzerland

⁵Department of Physiology and Biophysics, University of Washington School of Medicine, Seattle, WA 98195, USA

Summary

The kinesin-13 family member mitotic centromere-associated kinesin (MCAK) is a potent microtubule depolymerase [1–4]. Paradoxically, in cells it accumulates at the growing, rather than the shortening, microtubule plus ends. This plus-end tracking behavior requires the interaction between MCAK and members of the end-binding protein (EB) family [5–8], but the effect of EBs on the microtubule-destabilizing activity of MCAK and the functional significance of MCAK accumulation at the growing microtubule tips have so far remained elusive. Here, we dissect the functional interplay between MCAK and EB3 by reconstituting EB3-dependent MCAK activity on dynamic microtubules *in vitro*. Whereas MCAK alone efficiently blocks microtubule assembly, the addition of EB3 restores robust microtubule growth, an effect that is not dependent on the binding of MCAK to EB3. At the same time, EB3 targets MCAK to growing microtubule ends by increasing its association rate with microtubule tips, a process that requires direct interaction between the two proteins. This EB3-dependent microtubule plus-end accumulation does not affect the velocity of microtubule growth or shortening but enhances the capacity of MCAK to induce catastrophes. The combination of MCAK and EB3 thus promotes rapid switching between microtubule growth and shortening, which can be important for remodeling of the microtubule cytoskeleton.

Results

MCAK Tracks Growing Microtubule Ends *In Vitro* in an EB3-Dependent Manner

In vitro experiments with purified proteins have demonstrated that mitotic centromere-associated kinesin (MCAK) can function as a microtubule (MT) depolymerase and revealed the structural requirements for this activity [9–11]. However, these studies used Taxol- or GMPCPP-stabilized MTs rather than dynamic MTs, which represent the physiological substrate of

MCAK. To directly examine MCAK activity on growing MTs and explore the functional interplay between MCAK and EB3, we used an *in vitro* MT plus-end tracking assay [12]. MTs were grown in the presence of 15 μ M brain tubulin from GMPCPP-stabilized MT seeds [7, 13]. Purified fluorescent proteins added to the mixture were visualized using total internal reflection fluorescence microscopy; alternatively, MTs were imaged using differential interference contrast on the same microscope setup.

As was shown previously, EB3, one of three mammalian end-binding protein (EB) family members, fused to a fluorescent tag (N-terminal GFP or mCherry; see [13] and Figure 1A) prominently tracked growing MT ends [13]. The addition of 6 nM purified GFP-MCAK to dynamic MTs in the absence of EB3 blocked MT growth. In contrast, when 75–300 nM mCherry-EB3 was added together with GFP-MCAK, robust MT elongation episodes were observed (Figure 1B; see also Figure S1A and Movie S1 available online). In these conditions, GFP-MCAK bound to the MT lattice and showed enhanced accumulation at growing, but not depolymerizing, MT tips. This behavior was observed in the presence of ATP or ADP, indicating that ATP hydrolysis by MCAK is not required for plus-end tracking *in vitro* (Figure 1C). In agreement with previous observations [5], an MCAK mutant lacking the motor domain (GFP-MCAK-ML) was still able to track growing MT ends in the presence of mCherry-EB3 (Figure 1D). Based on these results, we conclude that EB3 can stabilize growing MTs against the MT-destabilizing activity of MCAK and at the same time target MCAK to the growing MT ends in a motor-independent manner. The protective activity of EB3 requires MT polymerization: in the absence of tubulin, 6 nM GFP-MCAK efficiently disassembled stabilized MT seeds even in the presence of 75 nM mCherry-EB3 (Figure S1B).

We next set out to address the importance of direct EB-MCAK interaction for the targeting of MCAK to growing MT plus-ends *in vitro*. A previous study showed that MCAK binds to the EBs through a linear motif, SKIP (denoted the SxIP motif), located in the N-terminal part of the molecule [7]. The SxIP motif fits into a cavity on the surface of the C-terminal EB1 homology (EBH) domain by establishing an extensive network of hydrogen bonds and hydrophobic contacts [7]. This cavity is in part shaped by the N-terminal half of the flexible C-terminal tail of the EBs (Figure S1C). Therefore, EB1 and EB3 deletion mutants lacking the entire C-terminal tails (EB1 Δ T and EB3 Δ T) failed to bind to GFP-MCAK (Figure S1D). Furthermore, simultaneous mutation of the EB3 residues Tyr226 and Glu234 to alanines (EB3-YE/AA), which is expected to disrupt hydrogen bond formation between the cavity at the EB3 C terminus and the SxIP peptide (Figure S1E), abrogated the interaction between MCAK and EB3 (Figure S1F). Importantly, the deletion of the tail or the YE/AA dual mutation did not affect the ability of EB3 to track growing MT ends (Figures 1E and 1F; [14]). However, its capacity to recruit GFP-MCAK to growing MT tips was abolished (Figures 1E and 1F; Movie S2). Finally, we made use of the fact that the change of the Ile97 and Pro98 residues of the MCAK SxIP motif to asparagines (MCAK-IP/NN) abolishes hydrophobic contacts of MCAK with the EBH domain [7]. The purified GFP-MCAK-IP/NN

*Correspondence: a.akhmanova@erasmusmc.nl

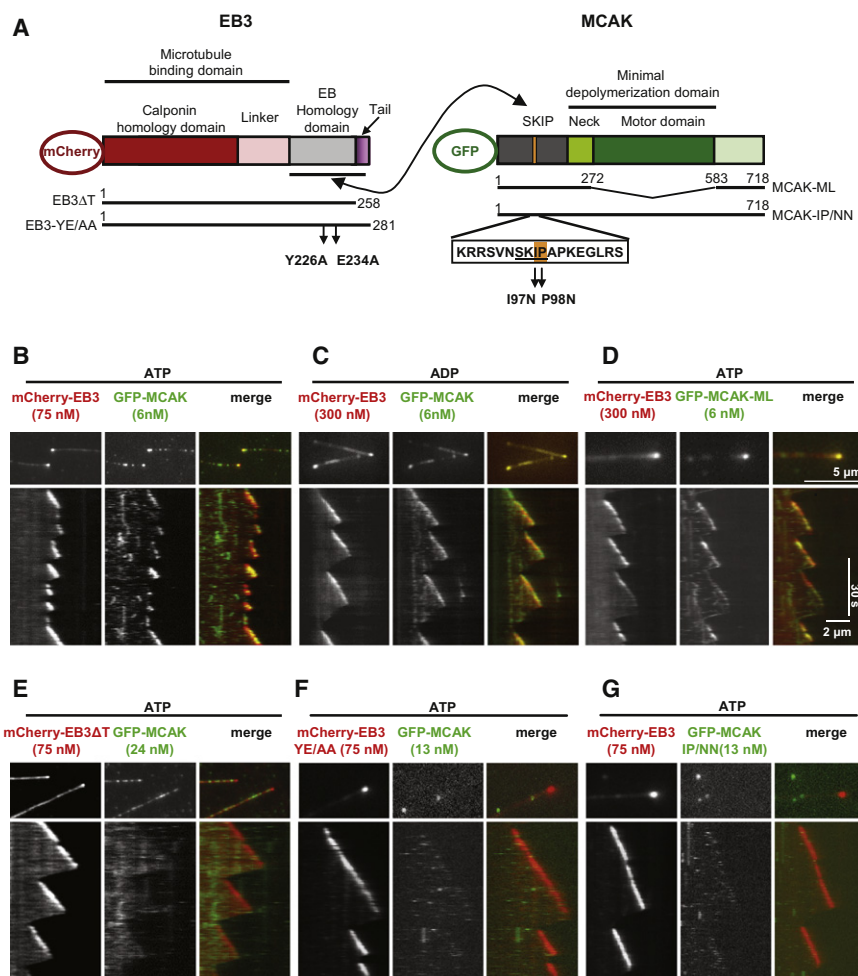


Figure 1. EB3 Is Necessary and Sufficient to Enable MCAK Plus-End Tracking In Vitro

(A) Schematic diagrams of EB3 and MCAK proteins and their mutants used in this study. The minimal microtubule depolymerization domain is based on [22]. The numbering is based on human EB3 (NCBI RefSeq ID NP_036458.2) and Chinese hamster MCAK (Swiss-Prot ID P70096).

(B–G) Total internal reflection fluorescence microscopy (TIRFM) images (top) and kymographs (bottom) of dynamic microtubules (MTs) grown in the presence of the indicated concentrations of GFP-MCAK and mCherry-EB3 or the indicated mutant proteins. Experiments in (B) and (D)–(G) were performed in the presence of 1 mM ATP; the experiment in (C) was performed in the presence of 1 mM ADP. Note that mCherry-EB3 Δ T showed an enhanced association with the MT lattice in addition to accumulation at the tip at concentrations above 100 nM. Therefore, 75 nM EB3 or EB3 mutants were used for all measurements of MT dynamics (Table S1; Figure 3A).

mutant failed to track MT plus ends in the presence of mCherry-EB3 in vitro (Figure 1G), further indicating that a direct EB-MCAK association is required to concentrate MCAK at the growing MT tips.

Analysis of MCAK and EB3 Dynamics by Single-Molecule Imaging

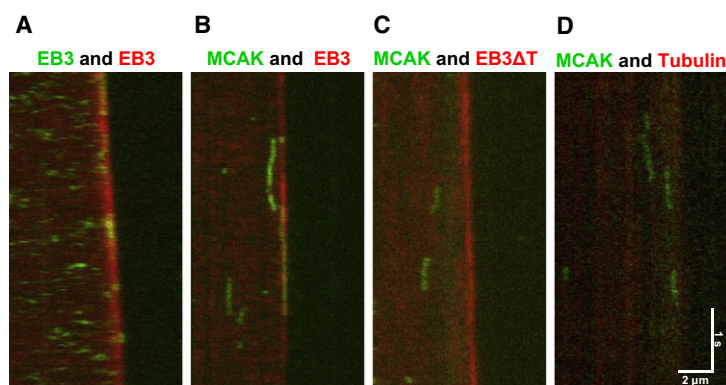
To determine the mechanism of MT plus-end tracking by MCAK in vitro, we characterized GFP-EB3 and GFP-MCAK turnover on growing MTs by fast single-molecule imaging (see Figure S2 for instrument calibration data and characterization of the fusion proteins). We performed the MT plus-end tracking experiments in the presence of subnanomolar concentrations of GFP-EB3 or GFP-MCAK and could reliably detect single GFP-EB3 or GFP-MCAK molecules on dynamic MTs. Initial prebleach intensities of these molecules displayed a nearly monodisperse distribution (Figures S2C and S2D). Simultaneous imaging of mCherry-EB3 was used to determine the position of the growing MT tip (Figures 2A–2C). As a control, we also imaged GFP-MCAK on growing rhodamine-labeled MTs in the absence of EB3 (Figure 2D).

From the single-molecule binding and unbinding events, we determined the association and dissociation rates for GFP-EB3 and GFP-MCAK (Figure 2E). GFP-EB3 showed an association rate almost three times higher and twice as long a dwell time on the MT tip compared to the MT lattice (Figure 2E; Figure S3); its dwell time on the MT end (0.3 s) was very similar

to that previously reported for the fission yeast homolog Mal3 (0.282 s) [12]. The association rate of GFP-MCAK was almost ten times lower than that of GFP-EB3 (Figure 2E). In the presence of full-length mCherry-EB3, GFP-MCAK showed an approximately 2-fold higher association rate with the MT tip compared to the lattice (Figure 2E). This effect was most likely due to a direct interaction between MCAK and EB3, because it was not observed with EB3 Δ T (Figure 2E). The dwell time of GFP-MCAK on MT tips in the presence of full-length mCherry-EB3 was also longer than that observed in the presence of mCherry-EB3 Δ T (Figure 2E; Figure S3). These results indicate that the interaction of MCAK with EB3 affects MCAK's association and possibly also its dissociation kinetics at dynamic MT tips.

Remarkably, the dwell times of GFP-MCAK on MT tips and the lattice exceeded those of GFP-EB3 by a factor of 3 to 4 (Figure 2E; Figure S3). A similar trend was previously observed for another EB binding partner, CLIP-170 [15, 16]. These observations might be explained by the fact that both MCAK and CLIP-170 interact not only with the EBs but also with the MT lattice, including tubulin E-hooks [10], and thus recognize composite binding sites. Nevertheless, the dwell times of both MCAK and EB3 were significantly shorter (0.3–1.2 s) than the comet decoration time (mean comet length divided by growth velocity), which was 9 ± 1 s for mCherry-EB3 and 10 ± 2 s for GFP-MCAK. This finding supports the view that the EBs and their partners, including MCAK, exchange rapidly on the binding sites at MT tips (dwell times of 1 s or less), whereas the sites themselves turn over relatively slowly (on the order of several seconds) [12, 17].

Next we examined one-dimensional diffusion of GFP-MCAK along the MT lattice and found that the diffusion coefficient of GFP-MCAK on dynamic MTs ($\sim 0.05 \mu\text{m}^2 \times \text{s}^{-1}$) was comparable to the one previously observed for the same GFP-MCAK preparation on Taxol-stabilized MTs ($\sim 0.08 \mu\text{m}^2 \times \text{s}^{-1}$) [11].



E

	Association Rate (n per 1 μm per 1 nM per 1 s)		Dwell Time (s)		Number of Events		Number of Experiments		Diffusion Coefficient on the lattice (μm ² s ⁻¹)
	Lattice	Tip	Lattice	Tip	Lattice	Tip	Lattice	Tip	
<u>EB3</u>	2.3 ± 0.9	6.5 ± 0.5	0.16 ± 0.03	0.34 ± 0.04	780	340	5	4	0.105 ± 0.008 (n = 1946)
<u>MCAK</u>	0.3 ± 0.11	ND	0.76 ± 0.08	ND	1026	ND	4	ND	0.047 ± 0.009 (n = 3544)
<u>MCAK + EB3</u>	0.4 ± 0.13	0.7 ± 0.3	0.66 ± 0.08	1.18 ± 0.29	1100	478	4	5	0.016 ± 0.003 (n = 581)
<u>MCAK + EB3ΔT</u>	0.2 ± 0.14	0.2 ± 0.13	0.54 ± 0.12	0.70 ± 0.35	1072	162	5	5	0.022 ± 0.002 (n = 541)

However, another study reported a value ~ 8 times higher [10], probably because of differences in protein preparations and experimental conditions. Interestingly, in the presence of mCherry-EB3 or mCherry-EB3ΔT, the diffusion coefficient of GFP-MCAK was further reduced (Figure 2E). This is unlikely to be due to the direct EB3-MCAK interaction, because both EB3 and EB3ΔT had a similar effect, and the diffusion coefficient of EB3 alone on the MT lattice was quite high ($\sim 0.1 \mu\text{m}^2 \times \text{s}^{-1}$). The reduced one-dimensional diffusion of MCAK might be explained by the molecular crowding on the MT lattice due to the presence of the EBs or by EB-induced changes in MT lattice structure [18, 19]. Taken together, our data demonstrate that the binding to the EBs governs MCAK association with MT tips and suggest that lateral diffusion might play a relatively minor role in the accumulation of MCAK at the EB-decorated growing MT ends.

A Combination of MCAK and EB3 Makes MTs Highly Dynamic

To analyze the functional consequences of the EB-MCAK interaction at the MT tips, we examined the combined effects of GFP-MCAK and mCherry-EB3 on MT dynamics. Increasing the concentration of GFP-MCAK from 6 to 12–13 nM almost completely blocked MT seed elongation in the presence of 75 nM full-length mCherry-EB3 (see below). In contrast, robust MT growth episodes were still observed in the presence of 75 nM mCherry-EB3ΔT or EB3-YE/AA (Figures 1E and 1F; Movie S2; data not shown).

Quantification of MT dynamics at different MCAK:EB3 ratios revealed that mCherry-EB3 alone increased the MT growth

Figure 2. Single-Molecule Imaging of GFP-EB3 and GFP-MCAK on Dynamic Microtubules

(A–D) Kymographs of dynamic MTs grown in the presence of mixtures of 0.3 nM GFP-EB3 and 75 nM mCherry-EB3 (A), 0.4 nM GFP-MCAK and 75 nM mCherry-EB3 (B), 0.4 nM GFP-MCAK and 75 nM mCherry-EB3ΔT (C), and 0.6 nM GFP-MCAK and rhodamine-labeled tubulin (D).

(E) Parameters of the GFP-EB3 and GFP-MCAK interactions with dynamic MTs. The experiments were performed in the presence of 75 nM mCherry-EB3 or mCherry-EB3ΔT in all cases except for GFP-MCAK alone, where rhodamine-labeled tubulin was added to visualize the MTs. The MT tip was defined as the area of bright staining with mCherry-EB3 or mCherry-EB3ΔT (typically, a 0.45 μm region at the MT end). Association rates were calculated from the total number of observed binding events; dwell times were calculated from dwell-time distributions (Figure S3) and corrected for photobleaching as described in [10] using the photobleaching time constant determined from the data shown in Figure S2E. The diffusion coefficient D was obtained from a weighted linear fit to the average of all squared displacement traces (excluding zero and up to the average binding time). Data are shown as mean \pm standard deviation (SD); SD represents variation between experiments for the association rate and the dwell time and represents the fitting error for the diffusion coefficient (numbers of analyzed traces are indicated in parentheses). ND indicates data values not determined because of a very low number of events and uncertainty in determining the MT tip area on rhodamine-labeled MTs.

rate as well as the catastrophe and rescue frequencies, similar to what we observed previously [13] (Figure 3A; Table S1). Remarkably, the addition of 6 nM GFP-MCAK affected only one MT dynamics parameter—the catastrophe frequency, which was increased 2-fold, whereas MT shortening and growth rates as well as the rescue frequency were unchanged (Figure 3A; Table S1). This indicates that the presence of MCAK at the growing MT tips has no effect on the growth phase so long as catastrophe is not induced, and that MCAK does not contribute to the depolymerization phase once it has started. In contrast, the addition of 6 to 24 nM GFP-MCAK-ML, which lacks the depolymerase activity, caused no increase in catastrophes, indicating that the enzymatic activity of MCAK is involved in catastrophe induction (Figure 3A; Table S1).

In the presence of mCherry-EB3ΔT, a 4-fold higher concentration of GFP-MCAK was required to induce a significant increase in MT catastrophe frequency (Figure 3A; Table S1). This finding correlates with the lower association rate and dwell time of MCAK at the MT tip in the presence of mCherry-EB3ΔT compared to mCherry-EB3. In contrast to what has been proposed previously [6], this result indicates that the direct interaction between MCAK and EB3 enhances the MT-destabilizing capacity of MCAK.

EB3 might promote MCAK-induced MT destabilization simply by concentrating MCAK at MT tips. Alternatively, by directly binding to MCAK, EB3 might act as an MCAK activator. In the latter case, a much lower concentration of MCAK at the MT tip would be needed to induce catastrophe in a situation when the wild-type MCAK and EB3 are added together, as

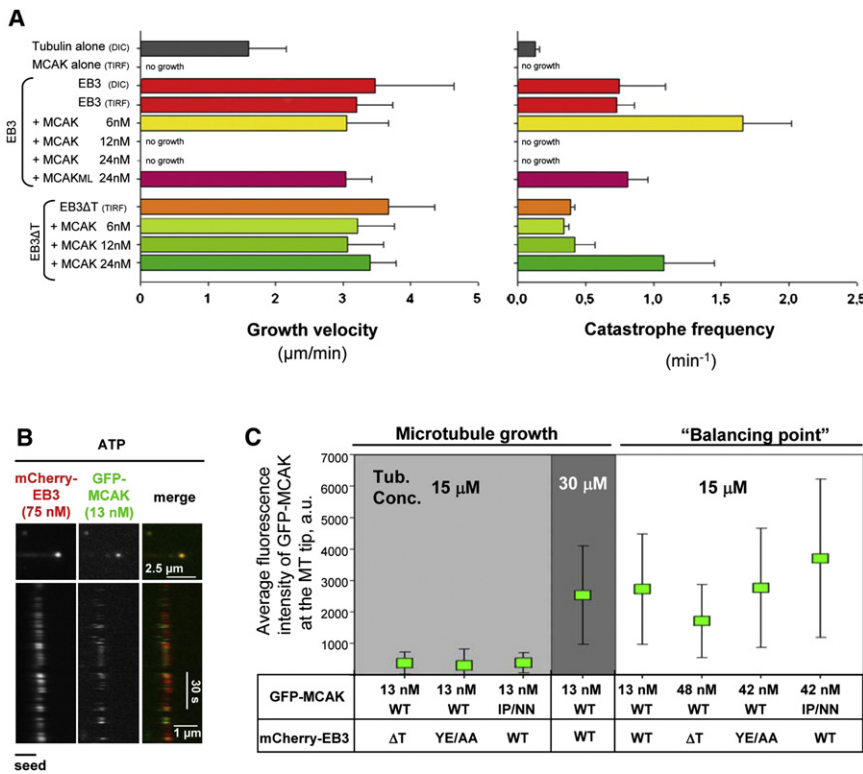


Figure 3. The Balance between MCAK and EB3 Concentrations Regulates Microtubule Plus-End Dynamics

(A) In vitro MT dynamics parameters, calculated from either differential interference contrast (DIC) or TIRFM movies as indicated, in the presence of tubulin either alone or with the addition of indicated concentrations of different protein combinations. Error bars represent SD. For growth velocities, SD was calculated from the total number of events (see Table S1). In case of transition frequencies, SD represents the variation between three experiments.

(B) Kymographs illustrating the “balancing point” conditions with 13 nM GFP-MCAK and 75 nM mCherry-EB3, at which MT seeds are not depolymerized but only very short MT growth events ($<0.5 \mu\text{m}$ in length) occur at the plus end of the seed.

(C) Fluorescence intensities of GFP-MCAK (in arbitrary units) at MT plus ends in conditions of MT growth (left) or at the balancing point (right), in the presence of 75 nM mCherry-EB3 (wild-type or indicated mutants) and the indicated concentrations of GFP-MCAK (wild-type or IP/NN mutant). The tubulin concentration used in the experiments is also indicated. Approximately 60–400 growth episodes from two or three independent experiments were analyzed for each condition. Error bars indicate SD.

opposed to any combination of mutant MCAK and EB3 in which the direct interaction between the two proteins is disrupted. To distinguish between these two possibilities, we used different combinations of wild-type or mutant GFP-MCAK and mCherry-EB3 proteins to determine the concentration of GFP-MCAK at which MT seed elongation was almost completely blocked, so that only very short MT outgrowth events with a length of less than $0.5 \mu\text{m}$ were observed (a state that we call the “balancing point”; Figure 3B). Importantly, the fluorescence intensity of GFP-MCAK at the MT tips was similar in all balancing-point conditions, irrespective of whether the particular combination of MCAK and EB3 proteins could interact with each other or not (Figure 3C). However, in all situations where the direct binding between MCAK and EB3 was abrogated, a 3- to 4-fold higher concentration of soluble GFP-MCAK was required to achieve the balancing point and the corresponding high level of GFP-MCAK intensity at MT tips (Figure 3C). These results indicate that EB3 enhances MCAK activity primarily by increasing its local concentration at the growing MT plus ends.

Interestingly, the balancing-point concentrations of GFP-MCAK in the presence of mCherry-EB3-YE/AA (which cannot bind MCAK) or GFP-MCAK-IP/NN (which is unable to interact with EB3) in the presence of wild-type mCherry-EB3 were the same (Figure 3C). This indicates that the IP/NN mutation, which is located outside of the MCAK neck and motor region (Figure 1A), has no significant effect on MCAK depolymerase activity and therefore primarily affects the ability of MCAK to be recruited to MT ends by EB3.

Next, we investigated whether MT growth at a given GFP-MCAK intensity at the MT tip could be rescued by increasing the tubulin concentration. Indeed, in the presence of 13 nM GFP-MCAK and 75 nM EB3, corresponding to the balancing point at $15 \mu\text{M}$ tubulin (Figure 3C), robust MT growth was

observed when the assay was performed with $30 \mu\text{M}$ tubulin. As expected, the polymerization rate increased in these conditions from $\sim 3\text{--}3.5 \mu\text{m}/\text{min}$ (Table S1) to $7.2 \pm 2.3 \mu\text{m}/\text{min}$ ($n = 68$). Importantly, the intensity of GFP-MCAK at the growing MT tips was similar to that observed with $15 \mu\text{M}$ tubulin (Figure 3C), indicating that a higher tubulin concentration and, consequently, a higher MT growth rate have a catastrophe-suppressing effect, in line with previously published data [20].

Interaction with EBs Makes MCAK a More Potent Depolymerase in Cells

We have previously shown that GFP-MCAK, but not GFP-MCAK-IP/NN, tracks growing MT ends in cells [7]. Next, we compared the capacity of the two proteins to destabilize cellular MTs. At high expression levels, the IP/NN mutant was capable of depolymerizing MTs to an extent similar to wild-type GFP-MCAK. However, at relatively low expression levels, a clear difference was observed: the wild-type GFP-MCAK caused a much more significant decrease in the number of MTs than the mutant (Figure 4). This result supports the idea that also in cells, the SxIP-mediated interaction of MCAK with EB3 concentrates MCAK on the MT tip and thus promotes MT destabilization.

Discussion

In this study, we reconstituted the functional interplay between EB3 and MCAK by using purified proteins on dynamic MTs, which represent the physiologically relevant substrate of MCAK. We found that EB3 counteracts MCAK by stabilizing the MT growth phase. This is an autonomous property of EB3, because it can be reconstituted in vitro in the absence of any MT-stabilizing EB partners. This conclusion is in

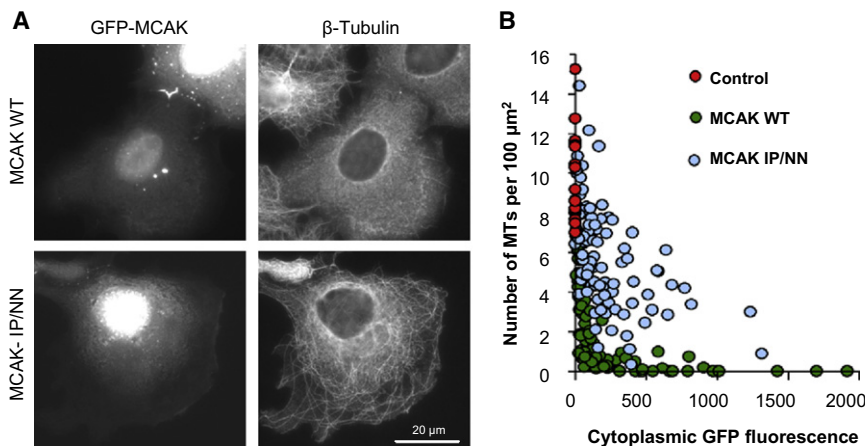


Figure 4. The SxIP Motif Mutant of MCAK Is a Less Efficient Microtubule Depolymerase Than the Wild-Type Protein

(A) COS-7 cells were transiently transfected with the indicated GFP fusions of human MCAK [7] and stained for β -tubulin 24 hr later. Note that the MT network is depolymerized in cells overexpressing wild-type GFP-MCAK, whereas it is still largely intact in cells overexpressing the GFP-MCAK-IP/NN mutant.

(B) Quantification of GFP-MCAK depolymerizing activity in COS-7 cells. Measurements were performed in untransfected cells (control) or in cells overexpressing wild-type GFP-MCAK or the IP/NN mutant. Each dot represents a measurement of the number of MTs per 100 μ m² in a single cell in relation to the average cytoplasmic GFP level after background subtraction.

agreement with our previous observations in cells, where EB proteins devoid of all partner-binding domains could still support processive MT growth [13]. In contrast, EBs cannot protect stabilizing MT lattice against MCAK-induced depolymerization (Figure S1B), in line with the fact that the kinetic parameters of their interaction with the growing MT tips and the mature lattice are different (Figure 2E).

In our reconstitution experiments, MCAK induced catastrophes but did not accumulate at the shrinking MT ends. Consistently, MCAK did not enhance the shortening rate of dynamic MTs. This suggests that MCAK depolymerase activity is only relevant for destabilizing a short region of a growing MT end; once a depolymerization event has been triggered, it proceeds spontaneously without further contribution of MCAK.

In addition, MCAK has a special relationship with EB proteins because they can concentrate it on growing MT tips, thus promoting MCAK-induced catastrophes. At first sight, this property seems counterintuitive—why would a MT-stabilizing protein target a depolymerase to MT ends? Our experiments provide clues to understand this paradox: carefully balanced concentrations of the two proteins result in robustly growing but highly dynamic MTs, a situation which might be exploited by the cells to promote rapid remodeling of MT arrays. Furthermore, the targeting of MCAK to MT ends through the same pathway that is also utilized by numerous MT stabilizers such as CLASPs, ACF7, or APC [21] might be beneficial by giving MCAK access to the MT tip in the crowded cellular environment. Finally, EB binding of MCAK can be negatively regulated by phosphorylation [7], making EB-dependent targeting of MCAK to the MT ends and its catastrophe-inducing activity susceptible to local and/or temporal regulation by different signaling pathways.

Supplemental Information

Supplemental Information includes three figures, one table, Supplemental Experimental Procedures, and two movies and can be found with this article online at doi:10.1016/j.cub.2010.08.020.

Acknowledgments

We thank C. Wyman (Erasmus Medical Center) for allowing us to perform atomic force microscopy in her laboratory. This work was supported by a Fundação para a Ciência e a Tecnologia fellowship to S.M.G., by Netherlands Organization for Scientific Research (NWO) ALW-VICI and ZonMw TOP grants to A.A., by an NWO ALW-VENI grant to L.C.K., and by NWO ZonMw-VIDI and European Science Foundation (European Young Investigators) awards to C.C.H. M.O.S. is supported by grants from the

Swiss National Science Foundation. R.M.B. acknowledges support by a Federation of European Biochemical Societies fellowship.

Received: March 29, 2010

Revised: July 30, 2010

Accepted: August 11, 2010

Published online: September 16, 2010

References

- Desai, A., Verma, S., Mitchison, T.J., and Walczak, C.E. (1999). Kin I kinesins are microtubule-destabilizing enzymes. *Cell* 96, 69–78.
- Wordeman, L. (2005). Microtubule-depolymerizing kinesins. *Curr. Opin. Cell Biol.* 17, 82–88.
- Howard, J., and Hyman, A.A. (2007). Microtubule polymerases and depolymerases. *Curr. Opin. Cell Biol.* 19, 31–35.
- Moores, C.A., and Milligan, R.A. (2006). Lucky 13-microtubule depolymerisation by kinesin-13 motors. *J. Cell Sci.* 119, 3905–3913.
- Moore, A.T., Rankin, K.E., von Dassow, G., Peris, L., Wagenbach, M., Ovechkina, Y., Andrieux, A., Job, D., and Wordeman, L. (2005). MCAK associates with the tips of polymerizing microtubules. *J. Cell Biol.* 169, 391–397.
- Lee, T., Langford, K.J., Askham, J.M., Brüning-Richardson, A., and Morrison, E.E. (2008). MCAK associates with EB1. *Oncogene* 27, 2494–2500.
- Honnappa, S., Gouveia, S.M., Weisbrich, A., Damberger, F.F., Bhavesh, N.S., Jawhari, H., Grigoriev, I., van Rijssel, F.J., Buey, R.M., Lawera, A., et al. (2009). An EB1-binding motif acts as a microtubule tip localization signal. *Cell* 138, 366–376.
- Mennella, V., Rogers, G.C., Rogers, S.L., Buster, D.W., Vale, R.D., and Sharp, D.J. (2005). Functionally distinct kinesin-13 family members cooperate to regulate microtubule dynamics during interphase. *Nat. Cell Biol.* 7, 235–245.
- Hunter, A.W., Caplow, M., Coy, D.L., Hancock, W.O., Diez, S., Wordeman, L., and Howard, J. (2003). The kinesin-related protein MCAK is a microtubule depolymerase that forms an ATP-hydrolyzing complex at microtubule ends. *Mol. Cell* 11, 445–457.
- Helenius, J., Brouhard, G., Kalaizidis, Y., Diez, S., and Howard, J. (2006). The depolymerizing kinesin MCAK uses lattice diffusion to rapidly target microtubule ends. *Nature* 441, 115–119.
- Cooper, J.R., Wagenbach, M., Asbury, C.L., and Wordeman, L. (2010). Catalysis of the microtubule on-rate is the major parameter regulating the depolymerase activity of MCAK. *Nat. Struct. Mol. Biol.* 17, 77–82.
- Bieling, P., Laan, L., Schek, H., Munteanu, E.L., Sandblad, L., Dogterom, M., Brunner, D., and Surrey, T. (2007). Reconstitution of a microtubule plus-end tracking system in vitro. *Nature* 450, 1100–1105.
- Komarova, Y., De Groot, C.O., Grigoriev, I., Gouveia, S.M., Munteanu, E.L., Schober, J.M., Honnappa, S., Buey, R.M., Hoogenraad, C.C., Dogterom, M., et al. (2009). Mammalian end binding proteins control persistent microtubule growth. *J. Cell Biol.* 184, 691–706.
- Komarova, Y., Lansbergen, G., Galjart, N., Grosveld, F., Borisy, G.G., and Akhmanova, A. (2005). EB1 and EB3 control CLIP dissociation from the ends of growing microtubules. *Mol. Biol. Cell* 16, 5334–5345.

15. Bieling, P., Kandels-Lewis, S., Telley, I.A., van Dijk, J., Janke, C., and Surrey, T. (2008). CLIP-170 tracks growing microtubule ends by dynamically recognizing composite EB1/tubulin-binding sites. *J. Cell Biol.* **183**, 1223–1233.
16. Dixit, R., Barnett, B., Lazarus, J.E., Tokito, M., Goldman, Y.E., and Holzbaur, E.L. (2009). Microtubule plus-end tracking by CLIP-170 requires EB1. *Proc. Natl. Acad. Sci. USA* **106**, 492–497.
17. Dragestein, K.A., van Cappellen, W.A., van Haren, J., Tsididis, G.D., Akhmanova, A., Knoch, T.A., Grosveld, F., and Galjart, N. (2008). Dynamic behavior of GFP-CLIP-170 reveals fast protein turnover on microtubule plus ends. *J. Cell Biol.* **180**, 729–737.
18. des Georges, A., Katsuki, M., Drummond, D.R., Osei, M., Cross, R.A., and Amos, L.A. (2008). Mal3, the *Schizosaccharomyces pombe* homolog of EB1, changes the microtubule lattice. *Nat. Struct. Mol. Biol.* **15**, 1102–1108.
19. Vitre, B., Coquelle, F.M., Heichette, C., Garnier, C., Chrétien, D., and Arnal, I. (2008). EB1 regulates microtubule dynamics and tubulin sheet closure in vitro. *Nat. Cell Biol.* **10**, 415–421.
20. Walker, R.A., O'Brien, E.T., Pryer, N.K., Soboeiro, M.F., Voter, W.A., Erickson, H.P., and Salmon, E.D. (1988). Dynamic instability of individual microtubules analyzed by video light microscopy: rate constants and transition frequencies. *J. Cell Biol.* **107**, 1437–1448.
21. Akhmanova, A., and Steinmetz, M.O. (2008). Tracking the ends: A dynamic protein network controls the fate of microtubule tips. *Nat. Rev. Mol. Cell Biol.* **9**, 309–322.
22. Maney, T., Wagenbach, M., and Wordeman, L. (2001). Molecular dissection of the microtubule depolymerizing activity of mitotic centromere-associated kinesin. *J. Biol. Chem.* **276**, 34753–34758.